Innovation of Combustion Particle Control Technologies Assisted by Numerical Modelling

Donato Rubinetti[1] Josef Wüest[2] OekoSolve AG[3]

***Abstract*—Worldwide efforts to promote the use of renewable energies include combustion-based technologies that produce substantial amounts of pollutants. In order to control the environmental impact a proper treatment of exhaust gases is required. This study describes the development of a numerical model for an electric filter which is being adapted to accelerate its R&D process.**

In the context of an industrially relevant project experimental data is obtained from a test rig and compared to the results from the simulation for validation purposes. Thus, further optimization and development of the electric filter is being carried out based on the presented modelling approach.

***Index Terms*—Particle Control, Combustion, Particle Deposition, Electric Filter.**

I. Introduction

In the light of worlwide efforts to promote renewable energy sources combustion-based technologies are increasingly being investigated. Due to the physical nature of combustion processes a considerable concentration of pollutants is released. The cleaning of exhaust gases is carried out by particle control devices such as electric filters. This study has been conducted in collaboration with *OekoSolve*, a Swiss producer of electric filters. The focus of the project is to improve and further develop the charging mechanism of an electric filter assisted by numerical modelling.

II. Physical Model

This study is a follow-up project of the *Electrostatic Precipitator* test-case presented in 2015 [1]. Apart from the geometry, the numerical and physical modelling practices are identical. In general, electric filters are used to both charge and accelerate particles. The acceleration triggers the deposition and removal of particles from exhaust gases. To obtain this effect in practice it is preferred to achieve a broad distribution of space charge density across the geometry of the electric filter. The relevant governing equations to model the distribution are Poissons equation (1)

$$\nabla^2\phi = -\frac{\rho_{el}}{\varepsilon_0} \tag{1}$$

and the transport equation for electric charge (2)

[1]Institute of Thermal and Fluid Engineering
University of Applied Sciences and Arts Northwestern Switzerland
e-mail: donato.rubinetti@fhnw.ch
[2]Institute of Bioenergy and Resource Efficiency
University of Applied Sciences and Arts Northwestern Switzerland
e-mail: josef.wueest@fhnw.ch
[3] web: oekosolve.ch
e-mail: info@oekosolve.ch

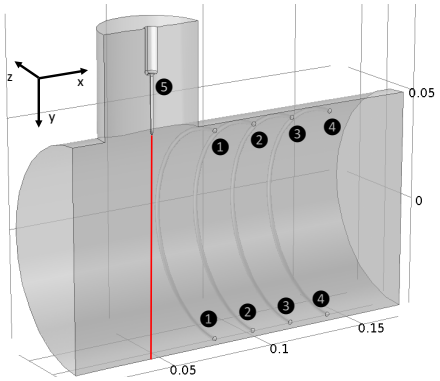

Fig. 1: 3D representation, units in [m]

Fig. 2: 2D representation, units in [m]

$$\boldsymbol{E}\nabla\rho_{el} = -\frac{{\rho_{el}}^2}{\varepsilon_0} \tag{2}$$

with ϕ being the electric potential, ρ_{el} being the space charge density, $\boldsymbol{E}$ being the electric field and ε_0 being the vacuum permittivity.

III. Numerical Model

The following numerical model is created using COMSOL Multiphysics 5.2a.

A. Approach

Due to its computationally expensive nature, the possibility to reduce the model to 2D is being investigated. Figures 3 to 5 compare the distributions of the electric field along the red cut line in figure 1 and 2. The radius is being noted as

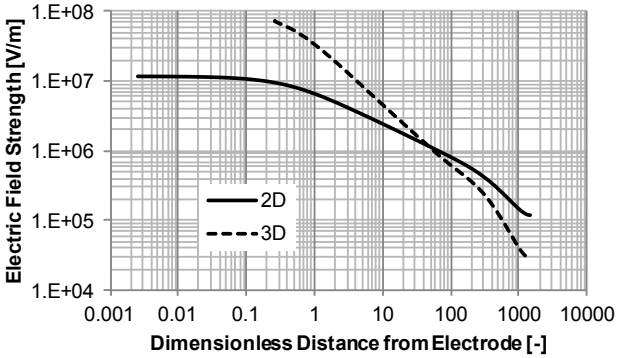

Fig. 3: Comparison of the Electric Field Magnitude

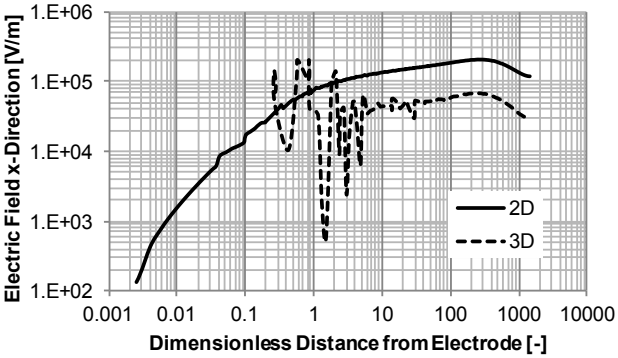

Fig. 4: Comparison of the Electric Field Strength horizontally (x-direction)

dimensionless by division by the electrode tip radius. It can be clearly seen, that

- the 2D case allows for a substantially finer mesh in proximity shown by the beginning point of the comparison curves (see also figure 6)
- the electric field as the driving quantity for electrical charge behaves in a similar way both in 2D and 3D in the relevant x and y spatial directions
- given figure 4 it can be observed that the electric field in x-direction in 3D is unreliable in proximity of the electrode due to the mesh size limitation

Thus, a 2D approach is suitable for a qualitative understanding of the model.

B. Boundary Conditions

The boundary conditions for the calculations are listed in table I. The voltage range is altered from -2kV to -30kV according to measurements, whereas the space charge density on the electrode is determined using the approach described in [1].

C. Mesh

Figure 6 shows the electrode cutout of the tetrahedral meshes used for the 3D and 2D computation. The 2D case allows the use of boundary layers in electrode proximity with

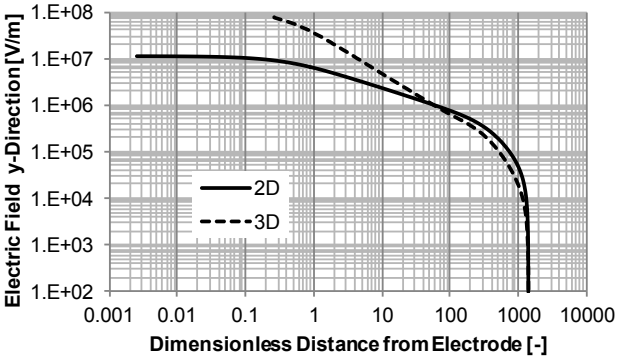

Fig. 5: Comparison of the Electric Field Strength vertically (y-direction)

Table I: Boundary conditions for the 2D and 3D simulations

Boundary	Part	2D	3D
1	Ring 1	ground	ground
2	Ring 2	ground	ground
3	Ring 3	ground	ground
4	Ring 4	ground	ground
5	Electrode	voltage & charge	voltage & charge

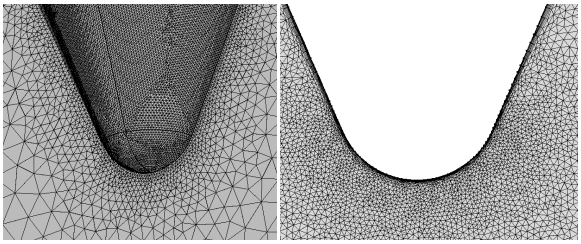

Fig. 6: 3D mesh in proximity of the electrode (left) and 2D mesh with boundary layers (right).

a total of approximately 300'000 cells, whereas the 3D case amounts to 1.6 million cells. The latter computes 40 hours on a Linux high-performance cluster, whereas the 2D case requires approximately a tenth of the computational effort.

D. Results

Figure 7 shows the results of the electric field which remains constant over most of the domain. However, the electric field lines indicate clearly that there is a decrease of intensity from ring 1 to ring 4. The crucial part of the process takes place in proximity of the electrode which can be observed in figure 8.

IV. Experimental Validation

A. Experimental setup and procedure

Figure 9 shows the experimental setup of the study. The emitting electrode is given a variable electric potential from negative 2kV to 30kV. Due to the ionization and acceleration of the plasma layer the electrical current can be observed and measured on the grounded rings M1-M4.

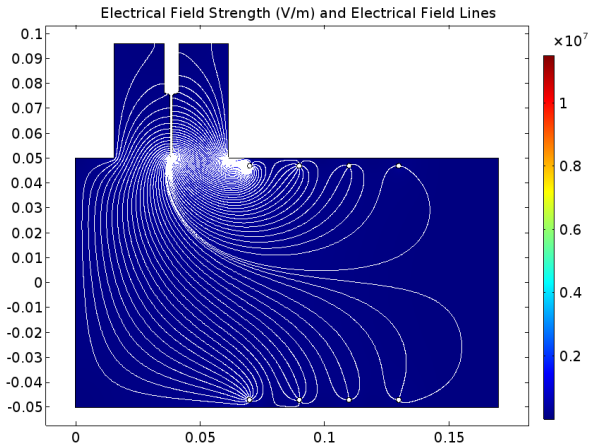

Fig. 7: 2D electrical field strength and electrical field lines

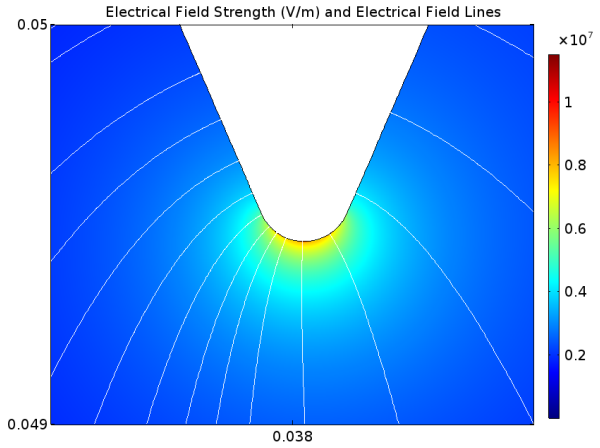

Fig. 8: 2D electrical field strength and electrical field lines close to the electrode

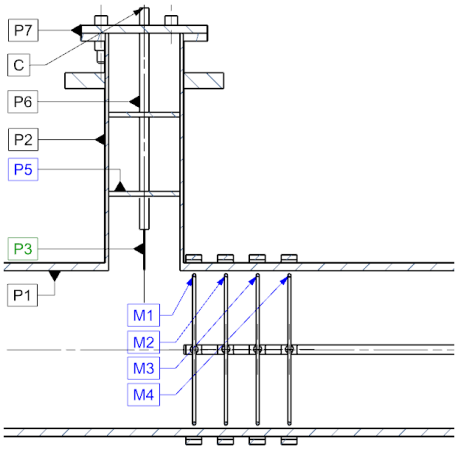

Fig. 9: Experimental setup with electrode P3 and measurement ring units M1 - M4. [2]

B. Results comparison

The measured electrical current in the experiment can only be compared to a certain extent to the computed 2D because

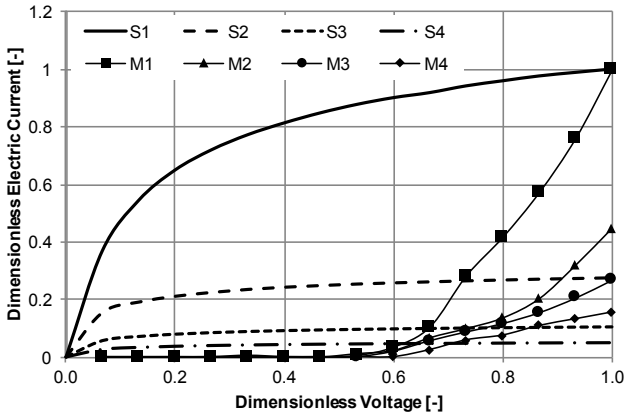

Fig. 10: Comparison of the simulation and measurements

of dimensional mismatch. In fact, the 2D computation yields a value in [A/m]. To show tendencies and enable a closer look, both results are being de-dimensionalized by division by the corresponding highest value obtained both for electric current and voltage. Figure 10 gives an overview of all measurements (M1-M4) and simulations (S1-S4). There is an ovious discrepancy between the results which can be explained by the aforementioned dimensional mismatch. Another point to reconsider is the setting of boundary conditions for the ground electrode. Even though the experiments are carried out in a Faraday cage, it is likely that the walls of the tube are grounded alongside with the rings. This circumstance distorts the electric field and affects the emitting capability of the electrode, which - as seen in figure 10 - has a relative onset voltage of ~ 0.6. However, it can be seen that in the simulation as well as in the measurements the first ring (S1,M1) significantly differs from the fellow rings which are closer to each another. This circumstance means that it is possible to qualitatively predict the behavior of physics when reduced to a 2D arrangement.

V. Conclusion & Outlook

A previously presented test-case model [1] has been adapted to an industrially relevant R&D project, showing the power of simulations for innovation purposes. The adaptation to this model comes with a series of modifications and a major simplification which is reducing a 3D phenomenon to a 2D case. The direct comparison between 2D and 3D cases show that particular care is needed to keep the physical accuracy. By acknowledging the limits and inconveniences created by this circumstance it is still possible to spot large optimization potential by qualitatively evaluating the tendencies in design changes. Figures 11 to 14 show four cases where the model undergoes parameter variations to facilitate the design optimization.

References

[1] Rubinetti, D. et al. (2015): *Electrostatic Precipitators - Modelling and Analytical Verification Concept.* COMSOL Conference 2015, Grenoble, 14-16 October.

[2] Hegyaljai, T. (2017): *Grundsatzversuche Sprühelektrode.* University of Applied Sciences and Arts, Northwestern Switzerland, Windisch.

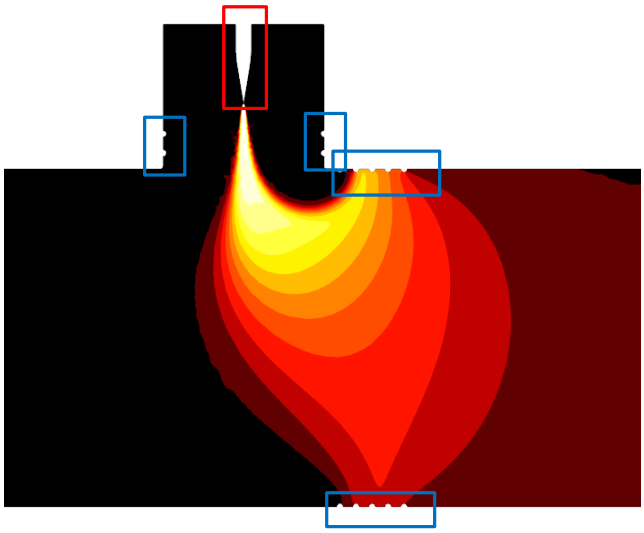

Fig. 11: Variation 1 - Needle -20kV, blue entities on ground. This configuration examines the possibility to focus and concentrate the beam of ionized air.

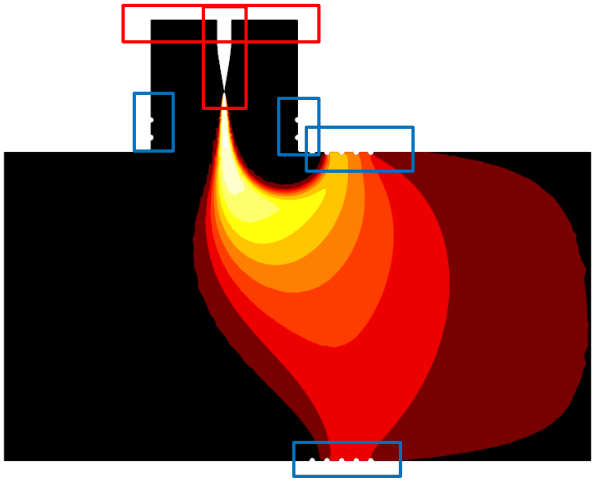

Fig. 13: Variation 3 - Needle and red entities -20kV, blue entities on ground. Similar to Variation 1 in figure 11 the beam does not greatly change shape when submitted to an additional backwards voltage.

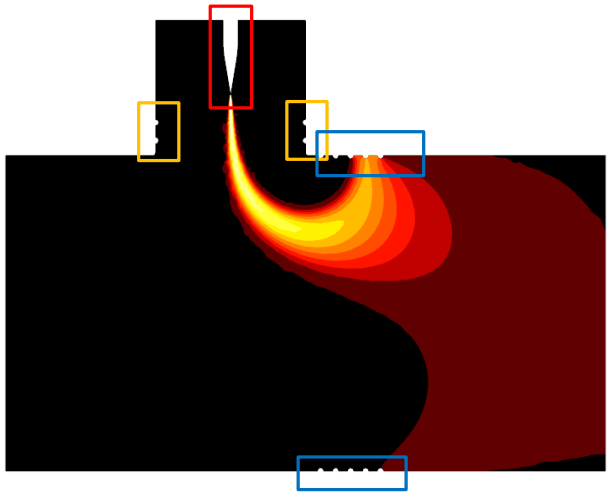

Fig. 12: Variation 2 - Needle -20kV, blue entities on ground, orange entities -5kV. When the needle is being assisted by additional electric fields generated by the orange entities, the ion beam is heavily distorted.

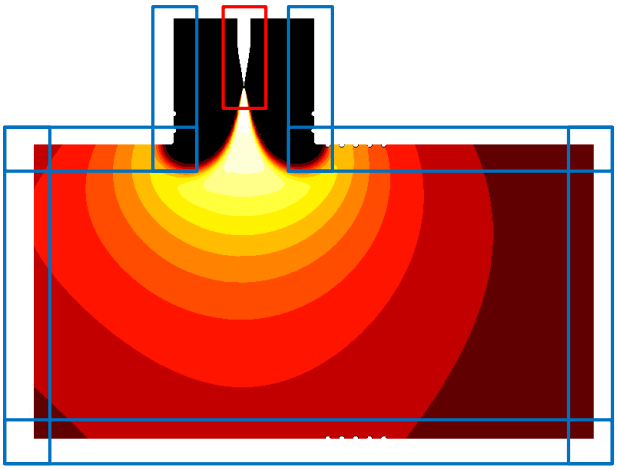

Fig. 14: Variation 4 - Needle -20kV, blue entities on ground. This variation shows exemplarily the strength of simulations when it comes to optimize the system. According to the prediction, when it is achievable to immerse the needle into a fully grounded domain it can be expected that the domain is vastly charged - which is desirable.